31st Annual International Conference of the IEEE EMBS
Minneapolis, Minnesota, USA, September 2-6, 2009

Design, Simulation and Fabrication of a Low Cost Capacitive Tactile Shear Sensor for a Robotic Hand

Arridh Shashank, *Student Member IEEE*, Mohsin I. Tiwana,
Stephen J. Redmond, *Member IEEE*, Nigel H. Lovell, *Senior Member, IEEE*

Abstract— **In this paper a novel shear sensor design is described. The proposed design is able to measure static shear forces. The sensor is fabricated on a printed circuit board and uses a differential capacitor arrangement to detect shear force applied to the sensor surface. Both mathematical and COMSOL models have been developed for the described sensor. The sensor is intended for use in robotic hands for the detection of shear force at the tactile interface. The device can be fabricated at a low cost in both low and high volumes. Prototype sensors with a ±0.525 mm displacement range were fabricated. Fixed displacements (over the range ±0.5 mm) are applied to the capacitor common plate, without a silicone covering, and a range of shear forces (over the range ±4 N) applied to the sensor, once covered with a silicone skin, and the differential capacitance of the transducer is recorded. The maximum standard deviation of the differential capacitance across all force values is 1.35e-15 F. The maximum standard deviation, at each force value, across a range of ±2 N is 4.28e-16 F.**

I. INTRODUCTION

It is often difficult to grasp and manipulate fragile and slippery objects with prosthetic or robotic arms. One significant problem faced is controlling the amount of grip force to apply. If the force applied is too small the object will slip, but too great a force will damage it. In a human hand, mechanoreceptors provide feedback and assist in controling the amount of force applied. However, it can be difficult to provide this feedback in a robotic hand because a single sensor is unable to compete with the thousands of afferent nerves present in the human finger pad. Typically, the glabrous skin of the hand is able to detect the distribution of forces and any changes therein. It has been shown that in a human model, localized incipient slip events provide information critical to controlling the amount of grip force exerted on the object being manipulated [11].

Studies have revealed that similar principles can be extended to a mechatronic model, to detect the onset of slip [8], [10]. Many other groups have undertaken significant research efforts towards the development of sensors designed to measure parameters such as normal and shear forces [2], [3], [4], [5], [6], [7], [8], [9]. The use of polyvinylidene fluoride (PVDF) for the detection of incipient slip has been well established [3], [6], [9] however PVDF alone is unable to transduce static force.

This research was support by an Australian Research Council Thinking Systems Grant.

The authors are with the Graduate School of Biomedical Engineering, University of New South Wales, Sydney, NSW 2052, Australia. n.lovell@unsw.edu.au

Some groups have attempted to overcome this by limitation using resistive [2], [7] or capacitive [4], [5] techniques. The employed resistive techniques have been shown to respond in a non-linear fashion [2]; furthermore they tend to lack resolution in their response in some cases [7]. Capacitance-based devices however have shown far greater promise. One particular design, fabricated using bulk-micromachining techniques, has been able to achieve spatial resolutions of 2.2 mm [4] per sensor device. However, the costs associated with this fabrication technique make it uneconomical for low volumes. A thin-film capacitive sensor has been proposed and shown to be effective, but it appears to lack the spatial resolution of other designs and is likely to prove difficult [5].

While a sensor capable of dynamically detecting slip is the desired endpoint, a sensor with the capacity to detect static shear forces may demonstrate some utility, where the coefficient of friction, between the tactile sensing surface and the object being manipulated, is known. This would allow for a suitable amount of normal force to be applied to the surface, as indicated by the shear force detected at the gripping interface. In this paper we present the initial design for a robust capacitive static shear force sensor, that can easily be produced at a low cost for all volumes. The sensor design is fabricated directly onto a printed circuit board (PCB). The device is characterized both with and without a silicone skin covering the capacitor plates.

II. METHODS

A. Structure and fabrication

The sensor consists of four independent elements, namely a top and bottom PCB, a flexible enameled copper ribbon and an elastomer. Fig. 1 depicts the top and cross-sectional views of the sensor. On the top PCB, a plated rectangular through hole pad is bisected on the long axis thus forming two capacitor plates. The bisection of the rectangular pad was achieved by using a 0.8 mm router bit. An enameled copper ribbon is threaded vertically down into the hole, where it becomes the common plate of a differential capacitor. The ribbon is anchored to the bottom PCB by soldering. In the prototype, the bottom PCB and the top PCB were fixed together and the signal conditioning circuitry was placed on the upper layer of the top PCB. The prototype sensor was fabricated with dimensions g = 1.2 mm, p = 0.15 mm, c = 3.0 mm, m = 3.5 mm, w = 0.8 mm and h = 1.6 mm. The w = 0.8 mm wide enameled copper ribbon used consisted of a 70 μm layer of copper coated with a 50

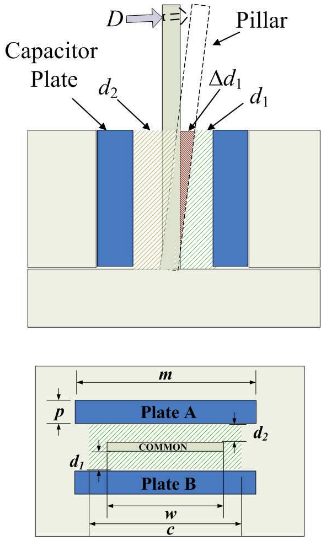

Fig. 1. The structure of the shear force sensor from side and top view. The top view also shows the displacement of the pillar when a force/displacement is applied. The diagram shows the sensor without its silicone coating.

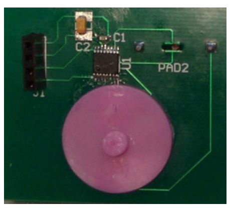

Fig. 2. Prototype board with bare sensor (PAD2). The second sensor is covered with pinkysil elastomer. The common plate of the second sensor is embedded within the nib of the pinkysil cover.

μm layer of polyamide and a 30μm layer of epoxy (total thickness: 150 μm). Polydimethylsiloxane (PDMS) based addition curing silicone elastomers of shore A hardness 20 (Pinkysil & Silpression, Barnes, Australia) was introduced into the space surrounding the copper ribbon to change the dynamic range of the sensor. Additionally, the elastomer was extended to form a raised silicone pillar over the surface of the PCB, as illustrated in Fig. 2. The PCBs were fabricated at a commercial PCB manufacturing facility. Where possible, solder masking was used to insulate the pad, however there was no solder mask on the façade of plates A and B.

B. Principle of operation

The sensor is a differential capacitor. The plated internal walls of the bisected pad form plates A and B of the capacitor. The enameled copper ribbon forms the common plate and stands as a vertical pillar between plates A and B. Deflections in the common plate vary the distances d_1 and d_2, thereby changing the measured capacitances as shown in Fig. 1.

C. Mathematical model

Upon application of force, F, the common plate experiences a displacement D, as shown in Fig. 1. This causes a negative change in Δd_1 on one side, while a positive change

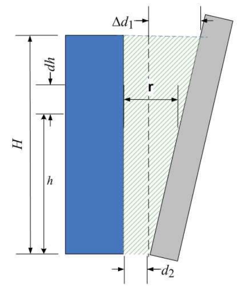

Fig. 3. Partial side-view of the sensor showing one plate and a displaced common plate due to shear force.

of Δd_1 occurs on the opposite plate, as shown in Fig. 3. Let w represent the width of all plates (depth into diagram). For parallel plate capacitors, capacitance can be expressed as:

$$C = \frac{A \in_0 \in_r}{r}$$

As shown in Fig. 3, for the small differential element of height dh at height h,

$$dC_1 = \in_0 \in_r wH \frac{dh}{Hd_1 - \Delta d_1 h}, \tag{1}$$

and

$$dC_2 = \in_0 \in_r wH \frac{dh}{Hd_2 + \Delta d_1 h}. \tag{2}$$

Hence for capacitance C_1 and C_2

$$C_1 = - \in_0 \in_r wH \left[\frac{\ln (Hd_1 - \Delta d_1 h)}{\Delta d_1} \right]_0^H, \tag{3}$$

$$C_2 = \in_0 \in_r wH \left[\frac{\ln (Hd_2 + \Delta d_1 h)}{\Delta d_1} \right]_0^H. \tag{4}$$

From (3) and (4), the differential capacitance, ΔC can be expressed as:

$$C_1 - C_2 = \in_0 \in_r wH \left[\frac{\ln \left[\frac{(d_1)(d_2)}{(d_1 - \Delta d_1)(d_2 + \Delta d_1)} \right]}{\Delta d_1} \right] \tag{5}$$

Equation 5 represents a simplified mathematical model of a differential plated capacitor, without accounting for fringing and parasitic effects.

D. Finite element analysis

In the second instantiation of the proposed sensor, the relationship between differential capacitance and force is considered, when the silicone covering is in place. Here we will simulate a shear force being applied to the silicone surface of a finite element model of the transducer structure. A comparison will later be made between this simulated model and a similar experiment performed upon the physical silicone covered sensor.

For pure electrostatic systems, Maxwell's equations relate electric charge contained in a Gaussian surface to the surrounding electric field by,

$$Q_i = \iiint_v \sigma dV = \in_r \in_0 \oiint \vec{E}(\vec{r}) d\vec{A}, \tag{6}$$

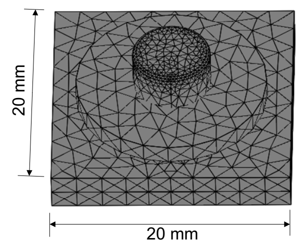

Fig. 4. Generated Mesh of Sensor.

and a derivable Poison's equation,

$$\in_0 \nabla \left[\left(\in_r (\vec{r}) \nabla \phi (\vec{r}) \right) \right] = -\sigma (\vec{r}) \tag{7}$$

Equation (6) can be used to calculate charge on a conductor in an electrostatic system. The differential capacitance expression for the system shown in (5) can compute this capacitance, but does not cater for the fringing effects in the capacitor, or the structural effects of the dielectric during structural deformations. Hence, a finite element analysis of the silicone covered sensor was performed using COMSOL. The Electrostatics (AC/DC Module), Moving Mesh (ALE) and Solid, Stress-Strain modules with Lagrange-Quadratic element types were used. A fine mesh with 40,508 tetrahedral elements and 111,144 degrees of freedom was generated as shown in Fig. 4. Simulation was done over the range ±4 N using the parametric solver.

E. Physical capacitance measurement

The sensor capacitance was measured using an Analog Devices AD7746 24-bit capacitance to digital converter chip operating in differential mode. The chip is able to measure dynamic changes in capacitance up to ±4.096 pF and can accommodate up to 17 pF of common-mode capacitance. The AD7746 has a maximum sampling rate of 90.9 Hz. The output of the analog-to-digital convertor (ADC) is sent serially to a Matlab GUI using a BASIC Stamp microcontroller.

1) Displacement micromanipulation without silicone skin: The sensor performance, without silicone skin, was measured experimentally. A micromanipulator with a 0.1 mm resolution and non-conductive tweezers were used to produce known displacements of the common plate. The capacitance was measured at intervals of 0.1 mm; each series of measurements contained 100 samples, acquired at a rate of 9.1 Hz.

2) Shear force application with silicone skin: The response of the sensor, with silicone skin, when subjected to a shear force was measured experimentally by fabricating a custom designed jig. The sensor was mounted on an inclined plane which could rotate between 0° and 90°. Fixed laboratory loads were placed on top of silicone nib. The weight had one normal and one shear component. The weights and angles were adjusted to obtain shear forces ranging from -4 N to +4 N, in 1 N steps. The forces were applied in a random sequence to obviate any memory effects in silicone.

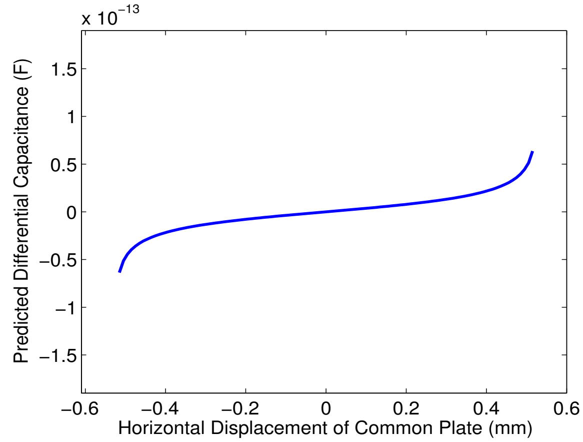

Fig. 5. Predicted sensor output for varying common plate displacements.

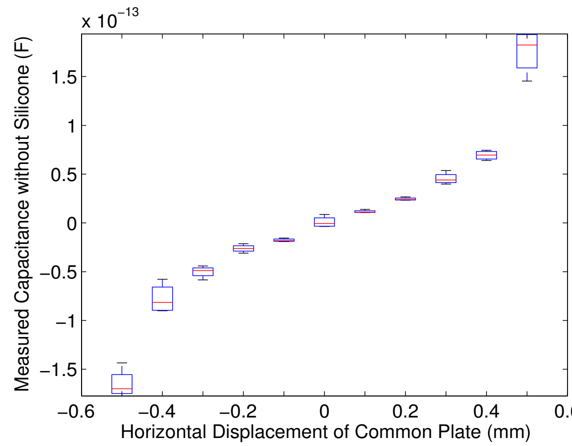

Fig. 6. Mean and standard deviation of the sensor output as measured experimentally without silicone.

III. Results

Fig. 5 illustrates the predicted differential capacitance for varying displacements of common plate without a silicone skin. The mean and standard deviation of the sensor output, measured experimentally, are shown in Fig. 6. Fig. 7 illustrates the mean capacitance and the standard deviation when the experiment was repeated six times with silicone. The standard deviation for full sensor range is 1.35E-15 which is much higher than the standard deviation at other load points. The maximum standard deviation, at each force value, across a range of ±2 N is 4.28e-16 F. In order to test the validity of the sub-domain and boundary conditions of our simulation model, an initial simulation was computed with a zero structural load. Simulation output capacitance between the common plate and one parallel conductor was 5.8021e-014 F compared to 5.1809e-014 F from the equation of parallel plate capacitance. The differential output capacitance of sensor with silicone skin is shown in Fig. 7.

IV. Discussion

The experimental results indicate that the sensor is able to transduce changes in displacement and shear force with a

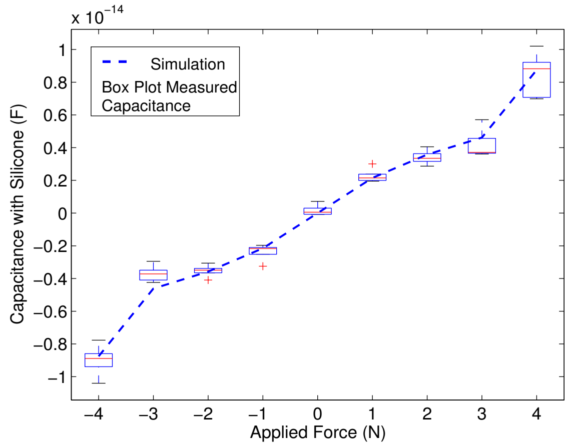

Fig. 7. Mean and standard deviation of the sensor output as measured experimentally with silicone along with simulation results.

relatively high repeatability. However in this initial design there seems to be significant variability in the measured signal at the extremes of the sensor range. It is hypothesized that this is due to unwanted deformation in the common plate as it contacts the edge plate and begins to buckle. It is also very likely that increasing the stiffness of the common plate would decrease the overall variability in the sensor output.

Noise did not pose a significant issue during experimentation, however it may become more significant if the overall dynamic capacitance of the system is reduced in order to make smaller versions of the sensor.

A slightly higher value from initial simulation with no structural load suggests that the simulation model caters for the electrostatic fringing which is not catered for in the mathematical model for the parallel plate capacitance. This also suggests the reason for a higher differential capacitance when measurements were performed without silicone. The differential output from the simulation closely matches with the actual measured response of the sensor shown in Fig. 7. Deviation between simulation results and actual measurements are observed at higher deformations.

Several problems were faced when using the silicone-based elastomers. These problems were mainly caused by the lack of adhesion between the silicone and the PCB which resulted in the silicone nib coming loose. The problem was solved by drilling small holes to allow the silicone to penetrate through the PCB and disperse on the bottom side thereby anchoring the nib structure more securely to the top side of the PCB. Similarly the sensor skin area was increased which gave increased adhesion between the sensor nib and PCB.

The sensor cost was reasonable when compared with the achievements of other groups [2], [4], [5]. In addition to the performance the device was fabricated at very low cost. The cost per unit when produced in low quantities is roughly $2 which is significantly lower when compared to other proposed devices [4]. It should also be noted, that although only two sensors were fabricated on the test board a low to medium density array of sensors can be fabricated using the same structure. Even marginal reductions in sensor dimensions should allow spatial resolutions of 3mm to be achieved.

V. Conclusion and Future Work

Overall this initial investigation indicated that the sensor presented in this paper is capable of providing the adequate resolution and range for the detection of shear force.

The fabricated sensor can be improved upon by reducing the dimensions and it is anticipated that future designs would be manufactured with pad sizes of approximately 1 mm. It is likely that this will reduce fringing effect as a result of the sensor design. The sensor design currently operates only along one axis, however by utilizing both channels of the capacitance to digital converter and dividing the PCB through hole pad into four sections, dual axis measurements can be acquired. It is also anticipated that a custom capacitance to digital conversion front-end would need to be developed to allow the simultaneous acquisition from an array of such sensors.

Future work will investigate the dynamic response of the sensor and its applications. COMSOL simulation models will be used to determine the optimum placement and density of sensor cells in the arrayed sensor. Analysis of sensor cross-talk, which is a major issue in arrayed sensors, can also be analyzed using this model. This will greatly aid in the development of arrayed sensors by avoiding the prototyping of different sensor densities and placement configurations.

References

[1] K. Arshak, D. Morris, A. Arshak, O. Korostynska, K. Kaneswaran, “Investigation into the pressure sensing properties of PVDF and PVB thick film capacitors”, *29th International Spring Seminar on Electronics Technology*, pp. 334-339, 2006.

[2] F. Zee, E. Holweg, W. Jongkind, G. Honderd, “Shear force measurement using a rubber based tactile matrix sensor”, 8^{th} *International Conference on Advanced Robotics,* pp. 733-738, 1997.

[3] J. Jockusch, J. Walter, H. Ritter, “A tactile sensor for a three-fingered robot manipulator”, *IEEE International Conference on Robotics and Automation*, pp. 3080-3086, 1997.

[4] Z. Chu, P. Sarro, S. Middelhoek, “Silicon three-axial tactile sensor”, *Solid-State Sensors and Actuators,* vol. A54, pp. 505-510, 1996.

[5] T. Chase, R. Luo, “A thin-film flexible capacitive tactile normal / shear force array sensor”, *IEEE International Conference on Industrial Electronics, Control, and Instrumentation*, pp. 1196-1201, 1995.

[6] J. Son, E. Monteverde, R. Howe, “A tactile sensor for localizing transient events in manipulation”, *IEEE Robotics and Automation*, pp. 471-476, 1994.

[7] L. Chen, S. Jin, T. Tiefel, “Tactile shear sensing using anisotropically conductive polymer”, *Applied Physics*, vol. 62, pp. 2440-2442, 1993.

[8] M. Tremblay, M. Cutkosky, “Estimating friction using incipient slip sensing during a manipulation task”, *IEEE Robotics and Automation,* pp. 429-434, 1993.

[9] R. Howe, “A tactile stress rate sensor for perception of fine surface features”, *Solid-State Sensors and Actuators*pp. 864-867, 1991.

[10] R. Howe, M. Cutkosky, “Sensing skin acceleration for slip and texture perception”, *IEEE International Conference on Robotics and Automation*, pp. 145-150, 1989.

[11] R. Johansson, G. Westling, “Roles of glabrous skin receptors and sensorimoter memory in automatic control of precision grip when lifting rougher or more slippery objects”, *Experimental Brain Research,*vol. 56, pp. 550-564, 1984.